DALTON
FULL PAPER

Dinuclear bis(bipyridine)ruthenium(II) complexes $[(bpy)_2Ru^{II}\{L\}^{2-}Ru^{II}(bpy)_2]^{2+}$ incorporating thiouracil-based dianionic asymmetric bridging ligands: synthesis, structure, redox and spectroelectrochemical properties

Soma Chakraborty,[a] Rebecca H. Laye,[b] Pradip Munshi,[a] Rowena L. Paul,[b] Michael D. Ward *[b] and Goutam Kumar Lahiri *[a]

[a] *Department of Chemistry, Indian Institute of Technology, Bombay, Mumbai-400076, India*
[b] *School of Chemistry, University of Bristol, Cantock's Close, UK BS8 ITS*

Received 11th February 2002, Accepted 20th March 2002
First published as an Advance Article on the web 29th April 2002

The reactions of $[Ru(bpy)_2(EtOH)_2]^{2+}$ with the asymmetric bridging ligands 2-thiouracil (H_2L^1) and 6-methyl-2-thiouracil (H_2L^2) in the presence of NEt_3 result in dinuclear complexes of the type $[\{(bpy)_2Ru\}_2(\mu\text{-}L)^{2-}]^{2+}$, where L = L^1 (complex $[\mathbf{1}]^{2+}$) and L^2 (complex $[\mathbf{2}]^{2+}$). In $[\mathbf{1}]^{2+}$ and $[\mathbf{2}]^{2+}$ the bridging functions act as a dinegative unit and bind with the two $[Ru(bpy)_2]^{2+}$ units through the terminal *N,S* and *N,O* donor sites. The crystal structure of the complex $[\mathbf{2}](ClO_4)_2$ has been determined. The structural parameters of complex $[\mathbf{2}](ClO_4)_2$ suggest a charge distribution with one negative charge associated with each binding site, which accordingly behave like a pyridonate and a thiopyridonate ligand. In acetonitrile, complex $[\mathbf{1}]^{2+}$ exhibits two reversible one-electron redox processes at half-wave potentials 0.17 (ΔE_p = 80) and 0.87 V (ΔE_p = 90 mV) *versus* SCE due to successive Ru(II)/Ru(III) couples. The successive Ru(II)/Ru(III) couples for $[\mathbf{2}]^{2+}$ appear at half wave potentials of 0.41 (ΔE_p = 200) and 0.72 V (ΔE_p = 100 mV) *versus* SCE. Both the complexes display a third oxidation process in the range 1.54–1.6 V *versus* SCE, which is ascribed to a process centred on the thiolato unit of the bridging ligand. The bipyridine based multiple reductions are observed in the range of −1.4 to −1.8 V *versus* SCE. The correlation between the structural parameters and the decrease in separation of the successive Ru(II)/Ru(III) couples while moving from $[\mathbf{1}]^{2+}$ (ΔE = 700 mV) to $[\mathbf{2}]^{2+}$ (ΔE = 310 mV) has been noted. A UV-Vis-NIR spectroelectrochemical study was carried out at 243 K on both the complexes. The mixed valence species $[\mathbf{1}]^{3+}$ and $[\mathbf{2}]^{3+}$ display broad intervalence charge-transfer transitions at 1170 nm and 1140 nm respectively, characteristic of class II complexes, which correspond to the electronic coupling constants V_{ab} of 950 cm^{-1} for $[\mathbf{1}]^{3+}$ and 900 cm^{-1} for $[\mathbf{2}]^{3+}$. The complexes are weakly luminescent at 77 K.

Introduction

The development of newer classes of polynuclear complexes in which Ru(II)–bpy fragments (bpy = 2,2′-bipyridine) are connected by bridging ligands is of continuing interest because of their outstanding electrochemical and/or luminescence properties.[1] In redox-active dinuclear complexes, the degree of intermetallic electronic communication depends principally on the nature of the bridging ligand: π-acceptor types of bridging ligands (often neutral, such as pyrazine), with a low-energy LUMO which is close in energy to the metal redox orbital, mediates the metal–metal electronic interaction *via* an electron-transfer mechanism in the mixed-valence state; in contrast electron-rich (often anionic) bridging ligands, in which the HOMO is close in energy to the metal redox orbitals, facilitate the intermetallic coupling by a hole-transfer mechanism.[2]

Although a wide variety of bridging ligands of both of the above types have been used in designing polynuclear ruthenium–bipyridine complexes in recent years,[2,3] the study of dinuclear complexes based on asymmetric bridging ligands, in which the two metal coordination sites are inequivalent, is less common.[4] In the present work we have investigated the ability of 2-thiouracil (H_2L^1) and 6-methyl-2-thiouracil (H_2L^2) to act as bis-bidentate bridging ligands capable of linking two $\{Ru(bpy)_2\}^{2+}$ units *via* the asymmetric bridge which presents an *N,S*-donor site to one metal ion and an *N,O*-donor site to the other. Thiouracils are minor component of tRNA in both *Escherichia coli* and mammalian tissues.[5] It has also been reported recently that thiouracil complexes possess effective antitumor and antiarthritic properties *in vivo*.[6] Thiouracil can function as a versatile ambidentate ligand, with coordination modes including monodentate *S*-donor,[7] bidentate chelating *N,S*-donor[8] or bridging *N,S*-donor,[9] amongst others. To the best of our knowledge only one metal complex, $[\{\eta^5\text{-}C_5H_4Me)_2Ti^{III}\}_2(2\text{-thiouracil})]$ is known where thiouracil bridges the two titanium ions through the terminal *N,S*- and *N,O*-donor sites.[10] Herein we report the syntheses, redox and spectroelectrochemical properties of the two dinuclear complexes $[\{(bpy)_2Ru\}_2(\mu\text{-}L)^{2-}]^{2+}$, where L = L^1 (complex **1**) and L^2 (complex **2**).

Results and discussion

Synthesis and characterisation of complexes

The reactions of 2-thiouracil (H_2L^1) and 6-methyl-2-thiouracil (H_2L^2) with the ruthenium precursor $[Ru(bpy)_2(EtOH)]^{2+}$ in the presence of NEt_3 under a dinitrogen atmosphere afford the dinuclear complexes $[\mathbf{1}]^{2+}$ and $[\mathbf{2}]^{2+}$ respectively, in which the bridging functions act as a dinegative unit and bind with the two $\{Ru(bpy)_2\}^{2+}$ units through the terminal *N,S* and *N,O*-donor sites (Scheme 1). The complexes were isolated as their trihydrated perchlorate salts; they exhibit satisfactory microanalytical data and display 1 : 2 conductivities in solution (experimental section). In addition, fast-atom bombardment mass spectra exhibited intense peaks centred at *m*/*z*, for $[\mathbf{1}](ClO_4)_2$: 1053 and 954 correspond to $[\mathbf{1}\{ClO_4\}]^+$ (calculated

 DOI: 10.1039/b201468h

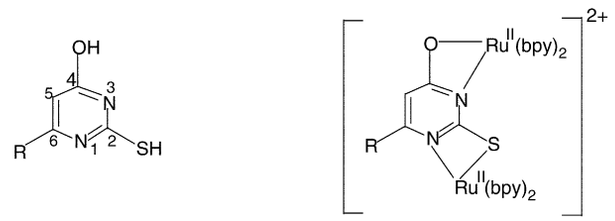

Scheme 1

value, 1052.47) and $[\mathbf{1}]^{2+}$ (calc. 953.02) respectively; and for $[\mathbf{2}](ClO_4)_2$: *m/z* 1067 and 967 correspond to $[\mathbf{2}\{ClO_4\}]^+$ (calc. 1066.50) and $[\mathbf{2}]^{2+}$ (calc. 967.05) respectively.

The ^{1}H NMR spectra of the complexes in CD_3CN are complicated in the aromatic region due to the presence of 32 inequivalent protons from the four bpy ligands. However, for $[\mathbf{1}](ClO_4)_2$ a doublet at 5.16 ppm (J = 7 Hz) arises from the H^5 proton of $(L^1)^{2-}$ which is coupled to H^6; the signal for H^6 is hidden under the bpy signals in the aromatic region (for free H_2L^1 in d^6-dmso, H^5 and H^6 occur at 5.8 and 7.4 ppm). For $[\mathbf{2}](ClO_4)_2$ this H^5 signal is a singlet at 5.40 ppm, and the methyl group at C^6 is apparent as a singlet at 1.07 ppm. The relatively high field position of this methyl signal may be explained with reference to the crystal structure (below), but the important point is that both complexes appear to exist as a single isomer in solution. Although three isomers are in principle possible due to the chirality of the tris-chelate metal centres,[11] it seems that one is sterically preferred, which is a common situation when the two metal centres are close together.[12]

The crystal structure of complex $[\mathbf{2}](ClO_4)_2\cdot H_2O$ is shown in Fig. 1; selected bond distances and angles are listed in Table 1.

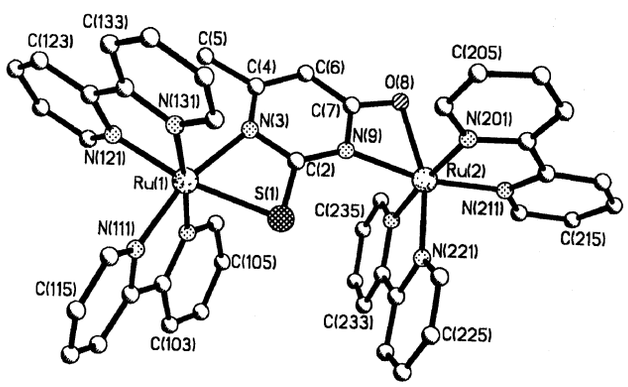

Fig. 1 Crystal structure of the complex cation of $[\mathbf{2}](ClO_4)_2\cdot H_2O$.

The bridging ligand $(L^2)^{2-}$ is doubly deprotonated, and act as an *N,O*-bidentate donor to Ru(2) and an *N,S*-bidentate donor to Ru(1), resulting in the formation of two four-membered chelate rings. Ru(1) and Ru(2) accordingly have irregular pseudo-octahedral N_5S and N_5O donor sets respectively, with the most marked deviations from octahedral geometry being associated with the small bite angles of the bidentate units within the four-membered chelate rings [68.57(9) and 62.54(11)° at Ru(1) and Ru(2) respectively]. The Ru ··· Ru separation is 5.88 Å; the two ruthenium ions are nearly coplanar with the bridging ligand, with distances out of the mean plane of $(L^2)^{2-}$ being 0.23 Å for Ru(1) and 0.35 Å for Ru(2) in the same direction.

Several possible tautomers of the deprotonated bridging ligands exist (Scheme 2, **A–D**).[13] The Ru–O and Ru–S separations cannot be used as reliable indicators of the charge distribution in the bridging ligand because of the particular steric effects associated with four-membered chelate rings in which

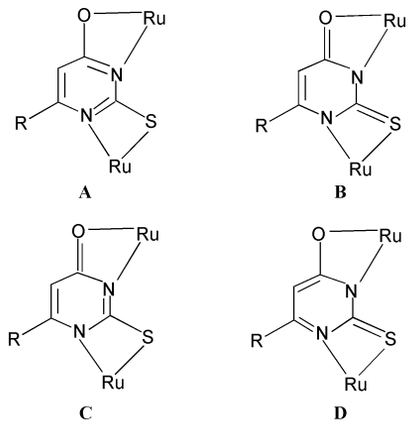

Scheme 2

the lone pairs of the two coordinating atoms are not convergent at the metal centre. At Ru(2) for example, if the Ru–N interaction is optimised then the Ru–O interaction cannot be and *vice versa*, which is why 2-pyridonate normally adopts a bridging coordination mode[14] (or occasionally a monodentate coordination mode)[15] in which this steric problem is avoided. Here, the Ru(2)–N(9) separation [2.070(3) Å] is in the normal range for Ru(II) coordinated to an aromatic N-heterocycle {*cf.* $[Ru(bpy)_3]^{2+}$, in which the Ru–N separations are 2.056 Å},[16] and consequently the Ru(2)–O(8) separation [2.170(3) Å] is elongated compared to typical unstrained Ru^{II}–O(phenolate) distances which are generally <2.1 Å.[16–19] A contrasting example was described by Tocher, in which a Ru(II)–(2-pyridonate) unit shows a 'normal' Ru–O distance but an elongated Ru–N distance.[20] At Ru(1), the Ru(1)–N(3) separation of 2.107(3) Å is rather long, but this could well be a separate steric effect associated with the nearby methyl group [C(5)] of the bridging ligand; for example, the presence of a substituent at the C^6 position of bpy is well known to result in the adjacent Ru–N separation being lengthened.[21] The Ru(1)–S(1) distance [2.4321(11) Å] is in agreement with those observed in related complexes with similar donor sets.[22] An additional important point is that the carbon atom of the methyl group on the bridging ligand [C(5)] lies near the face of the pyridine ring containing atoms N(121)–C(126) and is located 3.2 Å from the mean plane of this pyridine ring. This methyl group will accordingly be affected by the aromatic ring current, which accounts for the high-field position of its resonance in the ^{1}H NMR spectrum.

The bond distances *within* the ligand are more indicative than those around the metal centre of which tautomer(s) is/are present, as these distances are not subject to the steric influences which influence metal–ligand bond distances. For example, the C–O distance [1.288(4) Å] is considerably shorter than those found for phenolate donors with a formal C–O single bond (typically, 1.35 Å), but is in the range associated with a C–O bond order of 1.5.[23,24] The C–S distance [1.731(4) Å] is likewise somewhat less than a typical C(aromatic)–S single-bond distance, although not by as much,[23] and is actually very similar to those found in $[Ru(bpy)_2(2pyth)]^+$, where 2pyth is pyridine-2-thiol.[22] On this basis the ligand may be considered to lie somewhere between extremes **A** and **B**, which provides a charge distribution with one negative charge associated with each binding site, which accordingly behave like pyridonate and thiopyridonate ligands. Forms **C** and **D**, in which one metal ion coordinates to a neutral site and the other to a dianionic site, can be ruled out on common-sense as well as structural grounds. In fact, free 2-thiouracil (H_2L^1) exists in form **B** in the solid state with two NH protons.[25]

Redox properties of the complexes

The redox behaviour of the complexes was studied in acetonitrile solution by cyclic voltammetric and differential pulse

Table 1 Selected bond distances (Å) and angles (°) for $[2](ClO_4)_2 \cdot 2H_2O$

Ru(1)–N(111)	2.048(3)	Ru(2)–N(221)	2.021(3)
Ru(1)–N(101)	2.050(3)	Ru(2)–N(231)	2.034(3)
Ru(1)–N(121)	2.056(3)	Ru(2)–N(201)	2.043(3)
Ru(1)–N(131)	2.071(3)	Ru(2)–N(211)	2.045(3)
Ru(1)–N(3)	2.107(3)	Ru(2)–N(9)	2.070(3)
Ru(1)–S(1)	2.4321(11)	Ru(2)–O(8)	2.170(3)
C(2)–S(1)	1.731(4)	C(6)–C(7)	1.408(5)
C(7)–O(8)	1.288(4)	C(7)–N(9)	1.374(5)
C(4)–N(3)	1.359(5)	N(9)–C(2)	1.326(5)
C(4)–C(6)	1.367(6)	C(2)–N(3)	1.360(5)
N(111)–Ru(1)–N(101)	78.94(13)	N(221)–Ru(2)–N(231)	79.70(13)
N(111)–Ru(1)–N(121)	91.74(12)	N(221)–Ru(2)–N(201)	98.24(13)
N(101)–Ru(1)–N(121)	98.91(13)	N(231)–Ru(2)–N(201)	174.88(13)
N(111)–Ru(1)–N(131)	96.90(13)	N(221)–Ru(2)–N(211)	91.35(12)
N(101)–Ru(1)–N(131)	174.90(13)	N(231)–Ru(2)–N(211)	96.35(13)
N(121)–Ru(1)–N(131)	78.14(13)	N(201)–Ru(2)–N(211)	78.96(14)
N(111)–Ru(1)–N(3)	165.07(12)	N(221)–Ru(2)–N(9)	101.18(12)
N(101)–Ru(1)–N(3)	92.64(13)	N(231)–Ru(2)–N(9)	88.79(13)
N(121)–Ru(1)–N(3)	101.82(12)	N(201)–Ru(2)–N(9)	96.22(13)
N(131)–Ru(1)–N(3)	92.05(13)	N(211)–Ru(2)–N(9)	167.14(13)
N(111)–Ru(1)–S(1)	98.33(9)	N(221)–Ru(2)–O(8)	162.11(12)
N(101)–Ru(1)–S(1)	86.18(9)	N(231)–Ru(2)–O(8)	91.95(12)
N(121)–Ru(1)–S(1)	169.46(10)	N(201)–Ru(2)–O(8)	91.29(12)
N(131)–Ru(1)–S(1)	97.42(9)	N(211)–Ru(2)–O(8)	105.38(11)
N(3)–Ru(1)–S(1)	68.57(9)	N(9)–Ru(2)–O(8)	62.54(11)
C(2)–S(1)–Ru(1)	78.88(13)	N(221)–Ru(2)–C(7)	132.67(12)
C(4)–N(3)–C(2)	117.8(3)	N(231)–Ru(2)–C(7)	88.08(13)
C(7)–O(8)–Ru(2)	91.7(2)	N(201)–Ru(2)–C(7)	96.71(13)
N(9)–C(7)–C(6)	118.7(4)	N(221)–Ru(2)–C(7)	135.63(13)

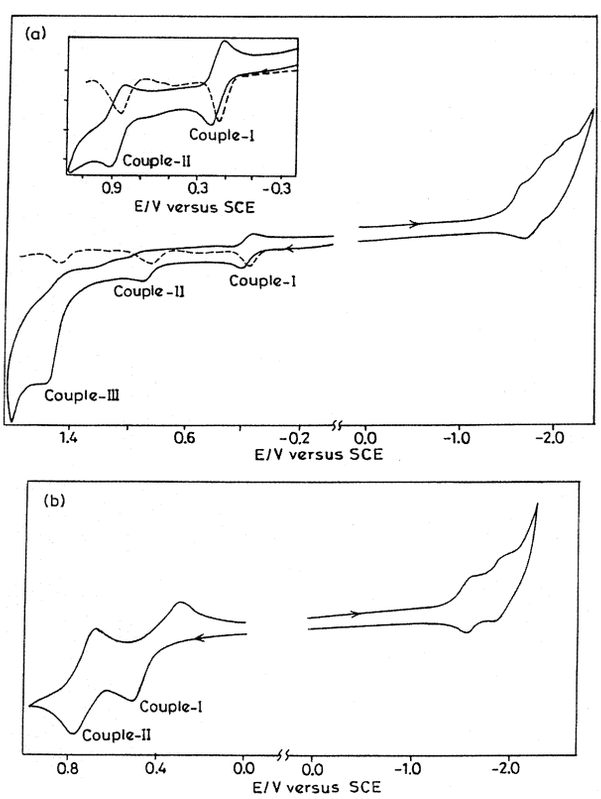

Fig. 2 (a) Cyclic voltammograms and differential pulse voltammograms in CH_3CN at a Pt-working electrode (for the positive side of SCE) and at a glassy-carbon working electrode (for the negative side of SCE) of $[1]^{2+}$ (the inset selectively highlights the couples I and II which indicate the reversible nature of couple II). (b) Cyclic voltammograms in CH_3CN at a Pt-working electrode (for the positive side of SCE) and at a glassy-carbon working electrode (for the negative side of SCE) of $[2]^{2+}$.

voltammetric techniques (Fig. 2). The oxidation processes at the positive side of the reference (SCE) were recorded by using a platinum working electrode. Reduction processes however were recorded by using a glassy carbon working electrode as the platinum working electrode failed to detect the reductions clearly.

Complex $[1]^{2+}$ exhibits two reversible one-electron redox processes at half-wave potentials 0.17 (ΔE_p = 80) and 0.87 V (ΔE_p = 90 mV), couples I and II respectively. The one-electron nature of couple I was confirmed by constant potential coulometry. These processes are assigned as stepwise Ru(II)/Ru(III) couples. In addition to these, $[1]^{2+}$ undergoes an irreversible oxidation at +1.54 V which we assign as a ligand-centred process based on the thiolate unit of $[L^1]^{2-}$;[26] also present are broad, poorly-defined processes at negative potentials (−1.40, −1.68 and −1.88 V) characteristic of bpy-based reductions.

The large separation of 700 mV between the Ru(II)/Ru(III) couples arises from a combination of the inherent difference in redox potentials associated with chemically different sites, and an electronic interaction mediated by the π-orbitals of the bridging ligand which results in a separation of the Ru(II)/Ru(III) couples on electrostatic grounds.[2] For the analogous mononuclear complexes $[Ru(bpy)_2(2\text{-}NC_5H_4O)]^+$ and $[Ru(bpy)_2(2\text{-}NC_5H_4S)]^+$, containing 2-pyridonate and 2-thiopyridonate donors respectively, the two Ru(II)/Ru(III) redox potentials are quite close, with that for $[Ru(bpy)_2(2\text{-}NC_5H_4S)]^+$ occurring at a potential 100 mV less positive than that for $[Ru(bpy)_2(2\text{-}NC_5H_4O)]^+$.[21] An exactly similar result is obtained from comparison of the redox properties of $[Ru(bpy)_2(2\text{-py-}C_6H_4O)]^+$ and $[Ru(bpy)_2(py\text{-}C_6H_4S)]^+$ (py = pyridine), where the Ru(II)/Ru(III) redox potential of the latter complex (with an N_5S donor set)[27] was 100 mV less positive than that of the former (with an N_5O donor set).[28]

Thus, for complex $[1]^{2+}$ we can say that (i) the Ru–N_5S site oxidises before the Ru–N_5O site; and (ii) much of the redox separation, possibly up to 600 mV, is ascribable to the electronic coupling through the bridging ligand. This is in the domain typically associated with strongly-interacting class III complexes with a delocalised mixed-valence state.[2] However, any asymmetry in the charge distribution in the complex will mean that the contribution to this redox separation from the asymmetry is increased, and that from the metal–metal coupling is reduced. In the two pairs of mononuclear model complexes mentioned above, in each case the *N,O*- or *N,S*-donor ligand has a charge of exactly −1 which is unlikely in $(L^1)^{2-}$; thus, the site

Table 2 Electronic spectral data (MeCN, 243 K)

Complex	λ_{max}/nm ($10^{-3}\varepsilon$/dm^3 mol^{-1} cm^{-1})
$[\mathbf{1}]^{2+}$	243 (58), 292 (98), 333 (19), 452 (13), 510 (sh)
$[\mathbf{1}]^{3+}$	244 (55), 283 (78), 397 (9.4), 438 (sh), 650 (1.1), 1170 (2.8)
$[\mathbf{2}]^{2+}$	242 (55), 292 (88), 342 (22), 499 (17)
$[\mathbf{2}]^{3+}$	245 (49), 283 (57), 360 (sh), 1140 (3.0)

asymmetry may be greater than expected on the basis of the mononuclear model complexes. As we see later, the spectroscopic properties of the mixed-valence state $[\mathbf{1}]^{3+}$ are actually characteristic of a class II mixed valence state.

The electrochemical behaviour of complex $[\mathbf{2}]^{2+}$ is rather different. Two processes are apparent which are assigned as Ru(II)/Ru(III) couples, at half-wave potentials of 0.41 and 0.72 V (couples I and II respectively). Of these, couple II appears to be a normal symmetric wave with ΔE_p = 100 mV in CH_3CN. Couple I however is abnormally broad in the cyclic voltammogram (ΔE_p = 200 mV), which is inconsistent with an electrochemically reversible process. We wondered if this behaviour could be due to an ec process (electron transfer followed by a chemical process) involving a CH_3CN solvent molecule, but exactly similar behaviour was observed in CH_2Cl_2 suggesting that the breadth of couple I might be ascribed to slow electron-transfer kinetics. Whatever the reason, coulometry confirmed that couple I corresponds to a 1-electron process, and UV-Vis-NIR spectroelectrochemistry (below) confirmed that the process is chemically reversible. In addition, a third (irreversible) oxidation at +1.61 V is ascribed to a process centred on the bridging ligand, as for $[\mathbf{1}]^{2+}$, and reversible bpy-centred reductions are apparent at high negative potentials (−1.57 and −1.84 V).

Following the reasoning used above for $[\mathbf{1}]^{2+}$, the first metal-centred oxidation (couple I) occurs at the Ru–N_5S site and the second (couple II) at the Ru–N_5O site. The electrochemical irreversibility of couple I appears to be linked to the steric hindrance associated with the presence of the methyl substituent on the bridging ligand, since this substituent is the only difference between the two complexes. This effect was clear in the crystal structure of $[\mathbf{2}](ClO_4)_2$ where the adjacent Ru–N bond (at the RuN_5S site) is elongated. The consequence of this distortion is a substantial reduction in the metal–metal coupling across the bridging ligand, with the 700 mV separation between Ru(II)/Ru(III) couples in $[\mathbf{1}]^{2+}$ being reduced to *ca.* 300 mV in $[\mathbf{2}]^{2+}$ (based on the separation between the centres of the two voltammetric waves). Compared to $[\mathbf{1}]^{2+}$ couple II (at the RuN_5O site) has shifted to lower potential by 150 mV, and the shift of couple I to higher potential is comparable. The magnitude of this difference is noteworthy. Derivatives of $[Ru(bpy)_3]^{2+}$ in which one of the Ru–N bonds is lengthened because of a bulky C^6 substituent on one of the ligands generally show only modest changes in the potentials of their Ru(II)/Ru(III) couples, because weakening one bond out of six has little overall effect on the coordination environment.[21,29] However since the bond that is weakened in $[\mathbf{2}]^{2+}$ is the one involving the bridging ligand π-system, the consequence for the electrochemical interaction is more substantial.

UV-Vis-NIR spectroelectrochemical properties

The spectroscopic properties of the complexes are summarised in Table 2 and the spectra are shown in Fig. 3. Both show, in their starting Ru(II)/Ru(II) state, moderately intense transitions in the 400–500 nm range which are ascribable to Ru[d(π)] ⟶ bpy(π*) MLCT transitions, and higher-intensity ligand-centred processes in the UV region; these are collectively unremarkable.[30]

Electrochemical oxidation of the bivalent complexes in CH_3CN at 243 K using a thermostatted OTTLE cell[31] generates the mixed-valence Ru(II)/Ru(III) species $[\mathbf{1}]^{3+}$ and $[\mathbf{2}]^{3+}$. In both cases the intensities of the Ru(II)-based MLCT transitions are

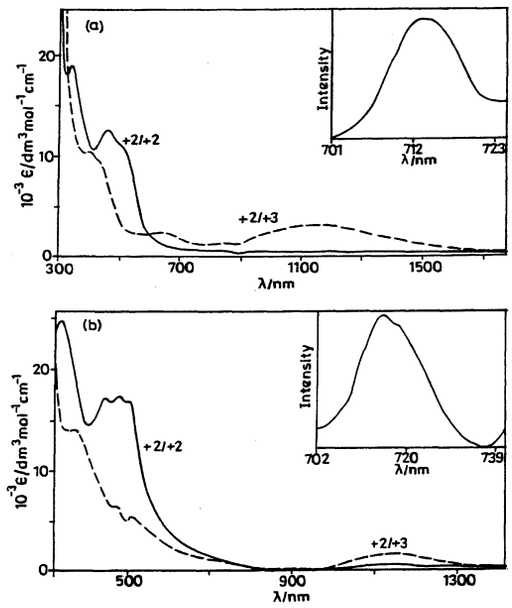

Fig. 3 Electronic spectra in CH_3CN at 243 K: (a) $[\mathbf{1}]^{2+}$ (—), $[\mathbf{1}]^{3+}$(- - -); (b) $[\mathbf{2}]^{2+}$ (—), $[\mathbf{2}]^{3+}$ (- - -). The insets show the emission spectra of $[\mathbf{1}]^{2+}$ and $[\mathbf{2}]^{2+}$ in 1 : 4 EtOH/MeOH at 77 K.

reduced and the relevant absorption maxima are blue-shifted. More significantly, in each case there is a new transition in the NIR region, at 1170 nm (ε 2800 dm^3 mol^{-1} cm^{-1}) for $[\mathbf{1}]^{3+}$ and 1140 nm (ε 3000 dm^3 mol^{-1} cm^{-1}) for $[\mathbf{2}]^{3+}$; the width at half maximum height for these is 3060 and 2400 cm^{-1} respectively. These are readily assignable as Ru(II) ⟶ Ru(III) inter-valence charge-transfer processes, and application of the Hush formula to this gives values of the electronic coupling constant V_{ab} of *ca.* 950 cm^{-1} for $[\mathbf{1}]^{3+}$ and 900 cm^{-1} for $[\mathbf{2}]^{3+}$.[32–34] Both of these are characteristic of class II complexes and the difference between them is scarcely significant, although we note that the fractionally weaker coupling in $[\mathbf{2}]^{3+}$ may be a reflection of elongated Ru–N bond to the bridging ligand which also resulted in a reduced separation between the redox potentials.

These values may be compared with the values of V_{ab} observed in $[\{Ru(bpy)_2Cl\}_2(\mu\text{-pym})]^{3+}$ and $[\{Ru(NH_3)_5\}_2(\mu\text{-pym})]^{5+}$, in both of which the bridging ligand is pyrimidine, having the same core structure as $(L^1)^{2-}$ and $(L^2)^{2-}$; the values are 150 cm^{-1} for $[\{Ru(bpy)_2Cl\}_2(\mu\text{-pym})]^{3+}$ in CH_3CN[35] and 145 cm^{-1} for $[\{Ru(NH_3)_5\}_2(\mu\text{-pym})]^{5+}$ in water.[34] The former case in particular provides a reasonable comparison with $[\mathbf{1}]^{3+}$ and $[\mathbf{2}]^{3+}$ since the donor set around each metal centre is comparable and the solvent is the same. The much stronger couplings observed for both $[\mathbf{1}]^{3+}$ and $[\mathbf{2}]^{3+}$ compared to the analogous pyrimidine-bridged complexes may be ascribed to the fact that the bridging ligand is a dianion rather than neutral, which will facilitate delocalisation by a hole-transfer pathway.[2,36] If a hole-transfer mechanism is operative, then the bridging ligand is transiently oxidised [Ru^{II}–L–Ru^{III} ⟶ Ru^{II}–L^+–Ru^{II} ⟶ Ru^{III}–L–Ru^{II}] during the delocalisation process. This would be facilitated by a relatively high-lying bridging ligand HOMO arising from the double negative charge, in contrast to the behaviour with neutral pyrimidine.[2] It has recently been demonstrated that an anionic bridging ligand is more effective than a neutral one in a pair of isomeric complexes at delocalising a Ru(II)/Ru(III) mixed-valence state for exactly this reason.[36]

Further oxidation of each complex to the Ru(III)–Ru(III) state resulted in disappearance of the IVCT transition, as expected. For $[\mathbf{1}]^{4+}$ an intense new transition at *ca.* 700 nm is ascribable to a LMCT process involving the Ru(III) centres. However, the doubly oxidised complexes both showed evidence of slow decomposition, so the spectra of $[\mathbf{1}]^{4+}$ and $[\mathbf{2}]^{4+}$ are not discussed further.

Luminescence behaviour

The complexes $[\mathbf{1}]^{2+}$ and $[\mathbf{2}]^{2+}$ are weakly luminescent (Fig. 3). Excitation of the complexes at the lowest energy MLCT band in methanol/ethanol (1 : 4) glass at 77 K results in emission maxima at 713 nm (quantum yield $\Phi = 6.8 \times 10^{-3}$) and 716 nm ($\Phi = 4.1 \times 10^{-2}$) for **1a** and **1b** respectively, with vibrational fine structures characteristic of emission from a ^{3}MLCT excited state involving the bipyridine ligand (Fig. 3, inset).[37]

Experimental

Materials

The starting complex *cis*-$[Ru(bpy)_2Cl_2]\cdot 2H_2O$ was prepared according to the reported procedure.[38] The ligands 2-thiouracil and 6-methyl-2-thiouracil were obtained from Aldrich, USA. Other chemicals and solvents were reagent grade and used as received. For electrochemical studies HPLC grade acetonitrile or CH_2Cl_2 was used. Commercial tetraethylammonium bromide was converted to pure tetraethylammonium perchlorate (TEAP, used as base electrolyte) by following an available procedure.[39]

Physical measurements

Solution electrical conductivity was checked using a Systronic conductivity bridge 305. Infrared spectra were taken on a Nicolet spectrophotometer with samples prepared as KBr pellets. UV-Vis-NIR spectroelectrochemistry studies were performed at 243 K in an optically transparent thin layer electrode (OTTLE) cell mounted in the sample compartment of a Perkin Elmer Lambda 19 spectrophotometer; the cell and the method used have been described previously.[31] ^{1}H-NMR spectra were obtained on a 300 MHz Varian FT-NMR spectrometer. Cyclic voltammetric and coulometric measurements were carried out using a PAR model 273A electrochemistry system. A platinum working electrode, a platinum wire auxiliary electrode and a saturated calomel reference electrode (SCE) were used in a standard three-electrode configuration. A glassy-carbon working electrode was used while recording the voltammograms at potentials negative of SCE. TEAP was the supporting electrolyte and the solution concentration was *ca.* 10^{-3} mol dm^{-3}; the scan rate used was 50 mV s^{-1}. A platinum gauze working electrode was used in coulometric experiments. All electrochemical experiments were carried out under dinitrogen atmosphere and all redox potentials are uncorrected for junction potentials. The elemental analyses were carried out with a Perkin-Elmer 240C elemental analyser. FAB mass spectra were recorded on a JEOL SX 102/DA-6000 mass spectrometer. Solution emission properties were checked using a SPEX-fluorolog spectrofluorometer, with fluorescence quantum yields being determined using a previously described method.[40]

Preparation of complexes $[\mathbf{1}](ClO_4)_2\cdot 3H_2O$ and $[\mathbf{2}](ClO_4)_2\cdot 3H_2O$

Both complexes were prepared by the same general procedure; the details are given for $[\mathbf{1}](ClO_4)_2\cdot 3H_2O$.

$[(bpy)_2Ru^{II}\{L^1\}Ru^{II}(bpy)_2](ClO_4)_2\cdot 3H_2O$, $[\mathbf{1}](ClO_4)_2\cdot 3H_2O$. The starting complex $[Ru(bpy)_2Cl_2]\cdot 2H_2O$ (100 mg, 0.19 mmol) and $AgClO_4$ (90 mg, 0.39 mmol) were taken in absolute ethanol (10 cm^3) and the mixture was heated to reflux with stirring for 1 h. The initial violet solution changed to orange–red; it was then cooled and filtered through a sintered-glass funnel. The ligand H_2L^1 (11 mg, 0.095 mmol) was then added to the above filtrate {containing $[Ru(bpy)_2(EtOH)_2]^{2+}$} followed by NEt_3 (19 mg, 0.38 mmol). The resulting mixture was refluxed overnight under dinitrogen. The precipitate which formed on cooling was filtered and washed thoroughly with cold ethanol. The product was recrystallised from acetonitrile–benzene (1 : 3). $[\mathbf{1}](ClO_4)_2\cdot 3H_2O$: Yield: 70% (80 mg); Anal. Calcd for $C_{44}H_{34}N_{10}Cl_2O_9SRu_2\cdot 3H_2O$: C, 43.8; H, 3.3; N, 11.6%. Found: C, 43.2; H, 3.0; N, 12.5%; Λ_M (Ω^{-1} cm^2 mol^{-1}) in acetonitrile at 298 K: 220. IR data: $\nu(ClO_4^-)$, cm^{-1}: 1103, 629.

For $[\mathbf{2}](ClO_4)_2\cdot 3H_2O$: Yield, 60% (69 mg). Anal. Calcd for $C_{45}H_{36}N_{10}Cl_2O_9SRu_2\cdot 3H_2O$: C, 44.3; H, 3.5; N, 11.5%; Found: C, 43.7; H, 3.1; N, 12.0%. Λ_M (Ω^{-1} cm^2 mol^{-1}) in acetonitrile at 298 K: 210. IR data: $\nu(ClO_4^-)$, cm^{-1}: 1098, 634.

Table 3 Crystallographic data for $[\mathbf{2}](ClO_4)_2\cdot H_2O$

Compound	**2**
Empirical formula	$C_{45}H_{38}Cl_2N_{10}O_{10}Ru_2S$
M_w	1183.95
Crystal system, space group	Monoclinic, *C*2/*c*
a/Å	33.660(5)
b/Å	15.466(2)
c/Å	21.098(3)
β/°	124.033(2)
V/Å^3	9102(2)
Z	8
T/K	173(2)
ρ_{calcd}/g cm^{-3}	1.728
Absorption coefficient/mm^{-1}	0.899
Data, restraints, parameters	10414/0/632
Final R_1, wR_2	0.0428, 0.0882

Crystallography

The single crystals of $[\mathbf{2}](ClO_4)_2\cdot H_2O$ were grown by slow diffusion of an acetonitrile solution of the complex into benzene, followed by slow evaporation. Significant crystal data collection and refinement parameters are listed in Table 3. X-Ray measurements were made at 173 K using a Bruker SMART CCD area-detector diffractometer with graphite-monochromated Mo-K_α radiation ($\lambda = 0.71073$ Å). An absorption correction was applied, based on multiple and symmetry-equivalent measurements.[41] The structure was solved by direct methods and refined by full-matrix least squares on weighted F^2 values for all reflections using the SHELX suite of programs.[42] All non-hydrogen atoms were assigned anisotropic displacement parameters and refined without positional constraints. All hydrogen atoms were constrained to ideal geometries and refined with fixed isotropic displacement parameters. The solvent (water) molecule was not assigned hydrogen atoms.

CCDC reference number 179291.

See http://www.rsc.org/suppdata/dt/b2/b201468h/ for crystallographic data in CIF or other electronic format.

Acknowledgements

Financial support received from the Council of Scientific and Industrial Research, New Delhi (India), the EPSRC (UK), and the Leverhulme Trust (UK) is gratefully acknowledged. Special acknowledgements are made to the Regional Sophisticated Instrumental Center (RSIC), Indian Institute of Technology, Bombay, for use of the NMR facility and Central Drug Research Institute, Lucknow (India) for the FAB-mass spectral data.

References and notes

1 V. Balzani, A. Zuris, M. Venturi, S. Campagna and S. Serroni, *Chem. Rev.*, 1996, **96**, 759; F. Scandola, M. T. Indelli, C. Chiorboti and C. A. Bignozzi, *Top. Curr. Chem.*, 1990, **158**, 73; E. S. Dodsworth, A. A. Vleek and A. B. P. Lever, *Inorg. Chem.*, 1994, **33**, 1045; E. Amouyal, *Sol. Energy Mater. Sol. Cells*, 1995, **38**, 249; A. Kay and M. Grätzel, *Sol. Energy Mater. Sol. Cells*, 1996, **44**, 99; R. Argazzi, C. A. Bignozzi, G. M. Hasselman and G. J. Meyer, *Inorg. Chem.*, 1998, **37**, 4533; V. Balzani and F. Scandola, *Supramolecular Photochemistry*, Ellis Horwood, New York, 1991; A. Hatzidimitriou, A. Gourdon, J. Devillers, J.-P. Launay, E. Mena and E. Amouyal, *Inorg. Chem.*, 1996, **35**, 2212; A. M. Barthram, R. L. Cleary, R. Kowallick and M. D. Ward, *Chem. Commun.*, 1998, 2695; F. Barigelletti and L. Flamigni, *Chem. Soc. Rev.*, 2000, **29**, 1;

F. Paul and C. Lapinte, *Coord. Chem. Rev.*, 1998, **178–180**, 431; M. D. Ward, *Chem. Ind.*, 1996, 568; M. D. Ward, *Chem. Ind.*, 1997, 640.
2 W. Kaim, A. Klein and M. Glöckle, *Acc. Chem. Res.*, 2000, **33**, 755; J. A. McCleverty and M. D. Ward, *Acc. Chem. Res.*, 1998, **31**, 842; D. Astruc, *Acc. Chem. Res.*, 1997, **30**, 383; M. D. Ward, *Chem. Soc. Rev.*, 1995, **24**, 121; R. J. Crutchley, *Adv. Inorg. Chem.*, 1994, **41**, 273; G. Giuffrida and S. Campagna, *Coord. Chem. Rev.*, 1994, **135–136**, 517.
3 R. Have, A. H. J. Dijkhuis, J. G. Haasnoot, R. Prins, J. Reedijk, B. E. Buchanan and J. G. Vos, *Inorg. Chem.*, 1988, **27**, 2185; R. Hage, J. G. Haasnoot, H. A. Nieuwenhuis, J. Reedijk, D. J. A. Ridder and J. G. Vos, *J. Am. Chem. Soc.*, 1990, **112**, 9245; S. Serroni, S. Campagna, G. Denti, T. E. Keyes and J. G. Vos, *Inorg. Chem.*, 1996, **35**, 4513; D. P. Rillema, R. Sahai, P. Matthews, A. K. Edwards, R. J. Shaver and I. Morgan, *Inorg. Chem.*, 1990, **29**, 167; M. Haga and A. M. Bond, *Inorg. Chem.*, 1991, **30**, 475; S. Baitalik, U. Florke and K. Nag, *J. Chem. Soc., Dalton Trans.*, 1999, 719; H. Masui, A. B. P. Lever and P. R. Auburn, *Inorg. Chem.*, 1991, **30**, 2402.
4 M. H. Chou, C. Creutz and N. Sutin, *Inorg. Chem.*, 1992, **31**, 2318; R. C. Rocha and H. E. Toma, *Inorg. Chim. Acta*, 2000, **310**, 65; A. E. Almaraz, L. A. Gentil, L. M. Baraldo and J. A. Olabe, *Inorg. Chem.*, 1997, **36**, 1517; F. Falgade and N. E. Katz, *Polyhedron*, 1995, **14**, 1213.
5 M. N. Lipsett, *J. Biol. Chem.*, 1965, **240**, 3975; J. A. Carbon, L. Hung and D. S. Jones, *Proc. Natl. Acad. Sci. USA*, 1965, **53**, 979; G. Thomas and A. Favre, *Biochem. Biophys. Res. Commun.*, 1975, **66**, 1454; L. G. Marzilli, *Prog. Inorg. Chem.*, 1977, **23**, 255; D. J. Hodgson, *Prog. Inorg. Chem.*, 1977, **23**, 211; B. G. Barrell and B. F. C. Clark, *Handbook of Nucleic acid Sequences*, Joynson Bruvvers, Ltd., Oxford, 1974.
6 P. D. Cookson, E. R. T. Tiekink and M. D. Whitehouse, *Aust. J. Chem.*, 1994, **47**, 577; E. R. T. Tiekink, P. D. Cookson, B. M. Linahan and L. K. Webster, *Met. Based Drugs*, 1994, 299.
7 E. C. Constable and P. R. Raithby, *J. Chem. Soc., Dalton Trans.*, 1987, 2281; G. W. Hunt, E. A. H. Griffith and E. L. Amma, *Inorg. Chem.*, 1976, **15**, 2993; D. J. Darensbourg, B. J. Frost, A. Derecskei-Kovacs and J. H. Reibenspies, *Inorg. Chem.*, 1999, **38**, 4715.
8 K. Yamanari, T. Nozaki, A. Fuyuhiro, Y. Kushi and S. Kaizaki, *J. Chem. Soc., Dalton Trans.*, 1996, 2851; K. Yamanari, T. Nazaki, A. Fuyuhiro and S. Kaizaki, *Chem. Lett.*, 1996, 35; K. Yamanari, S. Dogi, K. Okusako, T. Fujihara, A. Fuyuhino and S. Kaizaki, *Bull. Chem. Soc. Jpn.*, 1994, **67**, 3004; K. Yamanari, Y. Kushi, A. Fuyuhiro and S. Kaizaki, *J. Chem. Soc., Dalton Trans.*, 1996, 403.
9 S. Kitagawa, Y. Nozaka, M. Munakata and S. Kawata, *Inorg. Chim. Acta*, 1992, **197**, 169; D. M. L. Goodgame, R. W. Rollins, A. M. Z. Slawin, D. J. Williams and P. W. Zard, *Inorg. Chim. Acta*, 1986, **120**, 91.
10 D. R. Corbin, L. C. Francesconi, D. N. Hendrickson and G. D. Stucky, *J. Chem. Soc., Chem. Commun.*, 1979, 248.
11 N. C. Fletcher, T. C. Robinson, A. Behrendt, J. C. Jeffery, Z. R. Reeves and M. D. Ward, *J. Chem. Soc., Dalton Trans.*, 1999, 2999; N. C. Fletcher and F. R. Keene, *J. Chem. Soc., Dalton Trans.*, 1999, 683; N. C. Fletcher, P. C. Junk, D. A. Reitsma and F. R. Keene, *J. Chem. Soc., Dalton Trans.*, 1998, 133; T. J. Rutherford, O. V. Gijte, A. K. Mesmaeker and F. R. Keene, *Inorg. Chem.*, 1998, **37**, 645.
12 V. Balzani, D. A. Bardwell, F. Barigelletti, R. L. Cleary, M. Guardigli, J. C. Jeffery, T. Sovrani and M. D. Ward, *J. Chem. Soc., Dalton Trans.*, 1995, 3601; D. A. Bardwell, L. Horsburgh, J. C. Jeffery, L. F. Joulié, M. D. Ward, I. Webster and L. J. Yellowlees, *J. Chem. Soc., Dalton Trans.*, 1996, 2527; J. C. Jeffery, D. J. Liard and M. D. Ward, *Inorg. Chim. Acta*, 1996, **251**, 9.
13 J. M. Rawson and R. E. P. Winpenny, *Coord. Chem. Rev.*, 1995, **139**, 313.
14 E. P. Nelson and P. P. Phengsy, *J. Chem. Soc., Dalton Trans.*, 2000, 4023 and references therein.
15 D. P. Rillema, D. S. Jones and H. A. Levy, *J. Chem. Soc., Chem. Commun.*, 1979, 849.
16 N. Bag, A. Pramanik, G. K. Lahiri and A. Chakraborty, *Inorg. Chem.*, 1992, **31**, 40.
17 V. R. L. Constantino, H. E. Toma, L. F. C. de Oliveira, F. N. Rein, R. C. Rocha and D. O. Silva, *J. Chem. Soc., Dalton Trans.*, 1999, 1735.
18 S. Chakraborty, R. H. Laye, R. L. Paul, R. G. Gonnade, V. G. Puranik, M. D. Ward and G. K. Lahiri, *J. Chem. Soc., Dalton Trans.*, 2002, 1172.
19 S. Chakraborty, M. G. Walawalkar and G. K. Lahiri, *J. Chem. Soc., Dalton Trans.*, 2000, 2875.
20 J. W. Steed and D. A. Tocher, *J. Chem. Soc., Dalton Trans.*, 1992, 2765.
21 D. A. Bardwell, F. Barigelletti, R. L. Cleary, L. Flamigni, M. Guardigli, J. C. Jeffery and M. D. Ward, *Inorg. Chem.*, 1995, **33**, 2438; E. C. Constable, M. J. Hannon, A. M. W. Cargill Thompson, D. A. Tocher and J. V. Walker, *Supramol. Chem.*, 1993, **2**, 243.
22 B. K. Santra, M. Menon, C. K. Pal and G. K. Lahiri, *J. Chem. Soc., Dalton Trans.*, 1997, 1387; B. K. Santra, G. A. Thakur, P. Ghosh, A. Pramanik and G. K. Lahiri, *Inorg. Chem.*, 1996, **35**, 3050.
23 F. H. Allen, O. Kennard, D. G. Watson, L. Brammer, A. G. Orpen and R. Taylor, *J. Chem. Soc., Perkin Trans. 2*, 1987, S1.
24 C. G. Pierpont and R. M. Buchanan, *Coord. Chem. Rev.*, 1981, **38**, 44.
25 E. R. T. Tiekink, *Z. Kristallogr.*, 1989, **187**, 79; B. Kojic-Prodic, Z. Ruzic-Toros and E. Coffou, *Acta Crystallogr., Sect. B*, 1976, **32**, 1099; S. Swaminathan and K. K. Chacko, *Acta Crystallogr., Sect. B*, 1978, **34**, 3108; S. W. Hawkinson, *Acta Crystallogr., Sect. B*, 1975, **31**, 2153.
26 B. K. Santra and G. K. Lahiri, *J. Chem. Soc., Dalton Trans.*, 1997, 129; B. K. Santra and G. K. Lahiri, *J. Chem. Soc., Dalton Trans.*, 1997, 1883; B. K. Santra, P. Munshi, G. Das, P. Bharadwaj and G. K. Lahiri, *Polyhedron*, 1999, **18**, 617.
27 A. M. W. Cargill Thompson, D. A. Bardwell, J. C. Jeffery, L. H. Rees and M. D. Ward, *J. Chem. Soc., Dalton Trans.*, 1997, 721.
28 B. M. Holligan, J. C. Jeffery, M. K. Norgett, E. Schatz and M. D. Ward, *J. Chem. Soc., Dalton Trans.*, 1992, 3345.
29 R. H. Fabian, D. M. Klassen and R. W. Sonntag, *Inorg. Chem.*, 1980, **19**, 1977; J. M. Kelly, C. Lomg, C. M. O'Connell, J. C. Vos and A. H. A. Tinnemans, *Inorg. Chem.*, 1983, **22**, 2818.
30 A. Juris, V. Balzani, F. Barigeletti, S. Campagna, P. Belser and A. von Zelewsky, *Coord. Chem. Rev.*, 1988, **84**, 85.
31 S.-M. Lee, R. Kowallick, M. Marcaccio, J. A. McCleverty and M. D. Ward, *J. Chem. Soc., Dalton Trans.*, 1998, 3443.
32 The Hush formula for calculation of the electronic coupling V_{ab} from the parameters of an IVCT process is: $V_{ab} = \{[2.05 \times 10^{-2}(\varepsilon_{max}\ \bar{\nu}_{max}\ \Delta\bar{\nu}_{1/2})^{1/2}]/R\}$, where ε_{max}, $\bar{\nu}_{max}$, and $\Delta\bar{\nu}_{1/2}$ are the molar extinction coefficient, the absorption maximum in wavenumbers, and the bandwidth at half maximum height in wavenumbers, respectively (ref. 33); and R is the metal–metal distance in Å, taken as 5.88 Å from the crystal structure of [**2**]$(ClO_4)_2$.
33 N. S. Hush, *Coord. Chem. Rev.*, 1985, **64**, 135.
34 C. Creutz, *Prog. Inorg. Chem.*, 1983, **30**, 1.
35 M. J. Powers and T. J. Meyer, *Inorg. Chem.*, 1978, **17**, 2955; M. J. Powers and T. J. Meyer, *J. Am. Chem. Soc.*, 1980, **102**, 1289.
36 R. H. Laye, S. M. Couchman and M. D. Ward, *Inorg. Chem.*, 2001, **40**, 4089.
37 M. Vogler and K. J. Brewer, *Inorg. Chem.*, 1996, **35**, 818.
38 B. P. Sullivan, D. J. Salmon and T. J. Meyer, *Inorg. Chem.*, 1978, **17**, 3334.
39 D. T. Sawyer, A. Sobkowiak and J. L. Roberts, Jr., *Electrochemistry for Chemists*, Wiley, New York, 1995.
40 R. Alsfasser and R. van Eldik, *Inorg. Chem.*, 1996, **35**, 628; P. Chen, R. Duesing, D. K. Graff and T. J. Meyer, *J. Phys. Chem.*, 1991, **95**, 5850.
41 G. M. Sheldrick, SADABS, A program for absorption correction with the Siemens SMART system, University of Gottingen, Germany, 1996.
42 SHELXTL program system version 5.1, Bruker Analytical X-ray Instruments Inc., Madison, WI, 1998.